

Modelling and Fuzzy-Decision-Making of Batch Cultivation of *Saccharomyces cerevisiae* using Different Mixing Systems

M. Petrov* and T. Ilkova

Institute of Biophysics and Biomedical Engineering,
Bulgarian Academy of Sciences,
105 Acad. George Bonchev St., Sofia 1113, Bulgaria

doi: 10.15255/CABEQ.2014.2004

Original scientific paper

Received: February 19, 2014

Accepted: November 19, 2014

This study is focussed on the modelling and fuzzy-decision-making of *impulse mixing* and *vibromixing* for a *Saccharomyces cerevisiae* batch cultivation. Different substrate inhibition models (*Monod*, *Aiba*, *Andrews*, *Haldane*, *Luong*, *Edward*, and *Han-Levenspiel*) have been considered in order to explain the cell growth kinetics. The results obtained (correlation coefficient, Fisher coefficient, relative error and statistics I) show that all growth rate models are adequate and can be used for modelling. The investigations have shown that the most suitable for both mixing systems (according to the best statistical indicators) is the *Luong* growth rate model, which will be used for the process modelling. A fuzzy-decision-making procedure is developed with the initial conditions (maximal rotation speed for the *impulse mixing* and maximal amplitude for the *vibromixing* systems). The developed optimisation and results obtained have shown that the *impulse mixing* systems have better productiveness and better glucose assimilation. In addition, it is easier to realize this system.

Key words:

impulse mixing, vibromixing, modelling, fuzzy-decision-making, multiple objective optimisation, Pareto optimal solution, fuzzy sets theory

Introduction

Bioreactors which energy in a liquid and gas form is imported are universal in regard to management and establishment a definite mass exchange as mixing. In the mechanical mixing of the environment, the gas reaches its highest dispersion in the liquid as a result of the turbulence received. Having enough gas content, this may cause a huge relative surface of the phases contact; thus allowing the development of cultivation environments having components that differ significantly in respect to density. These advantages of stirred tank bioreactors (have led to their broad usage. They are mostly used in the production of enzymes, amino acids, antibiotics, etc.^{1,2}

However, for optimal cultivation performance, each specific system (culture + bioreactor) requires individual adjustment and optimisation of the cultivation conditions.³

In our study⁴, an alternative concept of the global models, namely *functional state modelling*, has been used. With this approach, the whole process is decomposed to *functional states*, each of which is described with a local model. The general disadvantage of this approach is that there are no clear criteria for understanding the phase of the pro-

cess and the great number of coefficients in the model. Therefore, it is unsuitable for optimization and optimal control.

Multiple objective optimisation is a natural extension of the traditional optimisation of a single objective function. On the one hand, if the multiple objective functions are commensurate, minimizing single objective function, it is possible to minimize all the criteria and the problem could be solved using traditional optimisation techniques. On the other hand, if the objective functions are incommensurate or competing, then the minimization of one objective function requires a compromise in another objective function. The competition between multiple objective functions is a key distinction between multiple objective optimisation and traditional single objective optimisation.^{5–7}

A Pareto optimisation technique has been used in study⁸ to locate the optimal conditions for an integrated bioprocessing sequence. The benefits of first reducing the feasible space by development provide a smaller search area for the optimisation.

Tonnon⁹ used an interactive procedure to solve multiple objective optimization problems (MOOP). A fuzzy sets theory (FST) has been used to model the engineer's judgment on each objective function. The properties of the obtained compromise solution

*Corresponding author: mpetrov@biomed.bas.bg

were investigated along with the links between the present method and those based on fuzzy logic.

In his works, Wang¹⁰ applies a fuzzy-decision-making procedure to find the optimal feed policy of a fed-batch fermentation process for fuel ethanol production using a genetically engineered *Saccharomyces* yeast as well as a fuzzy optimization of a two-stage fermentation process with cell recycling including an extractor for lactic acid production.

A method based on FST has been used for optimization of batch and fed-batch fermentation processes, as well as for optimization of gas-liquid mass-transfer in stirred tank bioreactors.^{11,12}

This study suggests a global model for modelling a process of different mixing types of the *Saccharomyces cerevisiae* cultivation. The concept of Pareto optimality is applied for finding a solution to MOOP. By using an assigned membership function for each of the objectives, the general multiple objective optimization problem (GMOOP) can be converted into a maximizing decision problem. In order to obtain a global solution, a FST method is introduced to solve the maximizing decision problem.

Material and methods

Experimental results

The deformation damage of the cells in the intensively mixed zones proved to be much more dangerous than the insufficient mass exchange in the so-called dead zones of the bioreactors. A special bioreactor design EDF5-30 was developed for simulation of these situations to provide producers sensitive to deformation forces with equally mixed cultivation conditions. The specific instruments BiO-3 and SiMD were developed for control of the process (www.bioreactors.net). BiO-3 allowed the control of all conventional parameters: temperature, pH, pO_2 , gas flow rate, shaft rotational speed, etc. SiMD measured the kinetic energy of flow fluctuations.

The experiments were realised in a batch culture (2 % glucose broth) of *Saccharomyces cerevisiae* in aerobic conditions (aeration – 1 L gas per 1 L broth).

A laboratory bioreactor EDF-5.3 was used in the experiments. It was equipped with a novel upper magnetic drive, bioprocess controller BIO-3 and SCADA (Fig. 1).^{13,14}

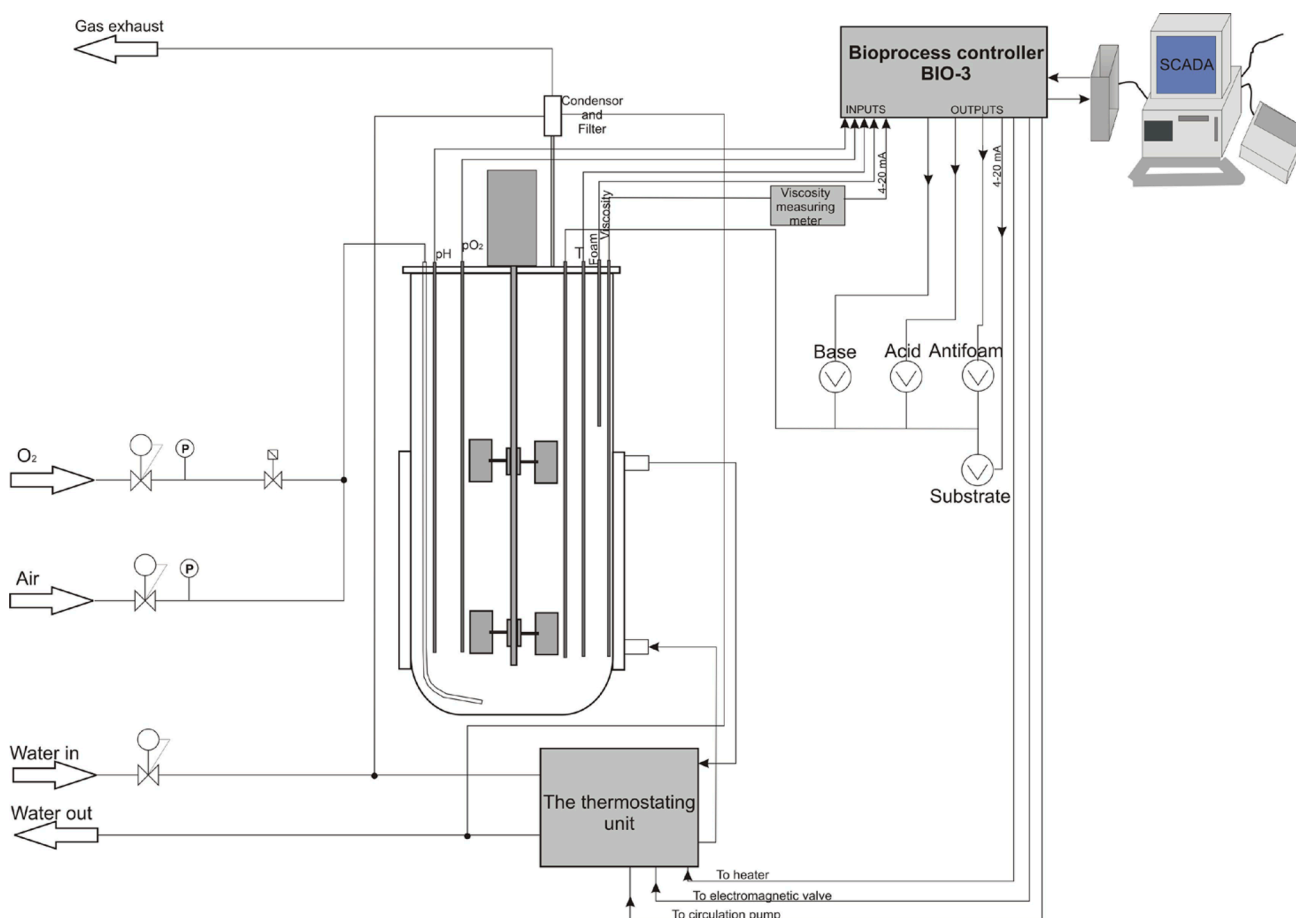


Fig. 1 – Schematic diagram of the fermentation process

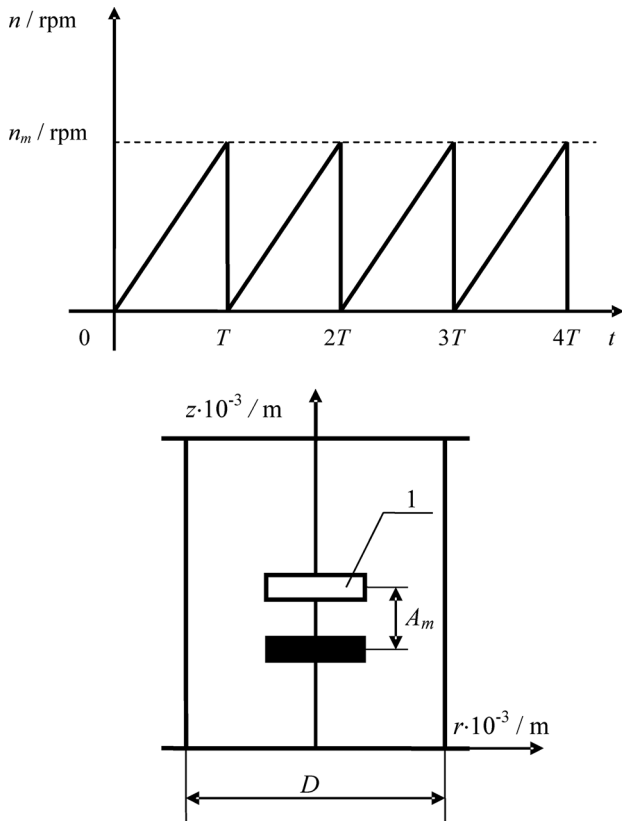


Fig. 2 – Realisation of the impulse and vibromixing systems; a) impulse mixing, where T is period, s ; n_m – maximal rotation speed, rpm; t – time, h; b) vibromixing, where l is vibrator plate; D – bioreactor diameter, m; A_m – amplitude, m; r – axis and z – axis

Two experiments^{4,14} were carried out in a bioreactor with a total volume of $5 \cdot 10^{-3} \text{ m}^3$ and a working volume $V = 3 \cdot 10^{-3} \text{ m}^3$. The *impulse mixing* system included a double Rushton turbine with baffles. The maximum rotation speed of the stirrer $n_m = 260 \text{ rpm}$ and mixing impulses had a frequency $f = 0.5 \text{ s}^{-1}$ and a period $T = 2 \text{ s}$ (Fig. 2a). The *vibromixing* was carried out by replacing the turbine stirrer with a vibrator plate, maximal amplitude $A_m = 10 \cdot 10^{-3} \text{ m}$ and frequency $f = 10 \text{ s}^{-1}$ (Fig. 2b).

Fig. 3 shows the results of the biomass and substrate concentration curves for the *Saccharomyces cerevisiae* cultivation using the impulse and vibromixing systems after applying a cubic spline procedure for experimental data.

As for the *impulse mixing*, the classic growing curve with a plateau region observed at the end of the process (Fig. 3), indicates that the substrate is completely used by the cells. This was confirmed by the glucose consumption rate (r_s) (Fig. 4).

The specific glucose consumption rate (R_s) curve (Fig. 5) shows that at the end of the process, this indicator of *impulse mixing* processes practically reaches zero, while for *vibromixing* conditions,

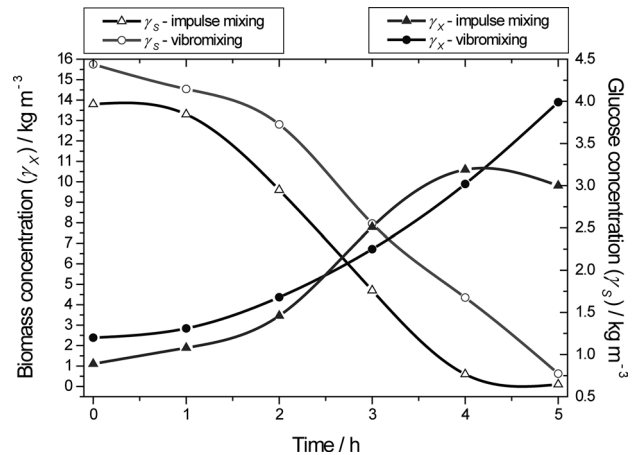


Fig. 3 – Experimental results for biomass and substrate concentration of *Saccharomyces cerevisiae*

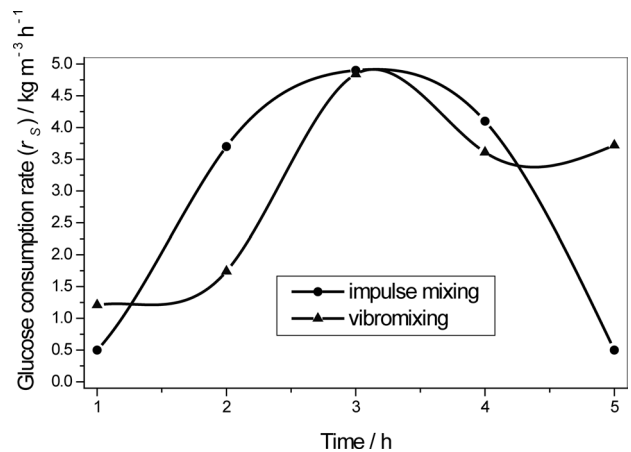


Fig. 4 – Glucose consumption rate (r_s) for the *Saccharomyces cerevisiae* growing process

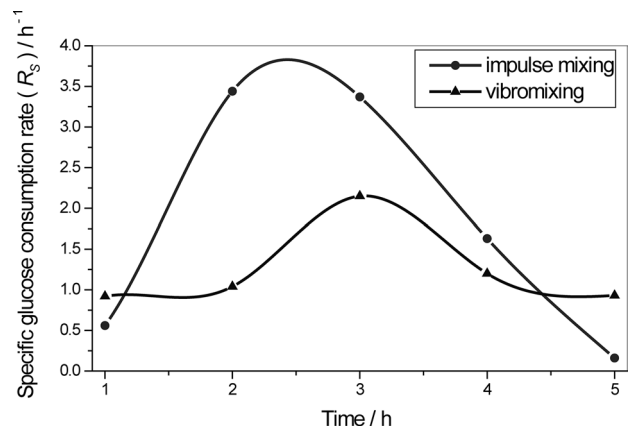


Fig. 5 – Specific glucose consumption rate (R_s) for the *Saccharomyces cerevisiae* growing process

the curve of the specific glucose consumption rate, increases only in the third hour of cultivation.

When the yeast growing process was analysed using the specific growth rate (μ) of the culture, the curves show (Fig. 6.) that by using a Rushton turbine with *impulse mixing*, microorganism growth is rapid in the first three hours after which the rate of

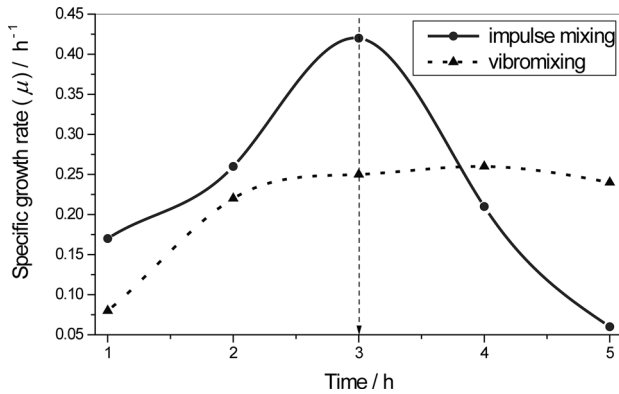


Fig. 6 – Specific growth rate (μ) of *Saccharomyces cerevisiae*

the process decreases. This can be explained by the decrease of substrate concentration and slower mass exchange. For vibromixing conditions, at the beginning of the process, the value of the specific growth rate increases in the first two hours, after which changes are minor.

One of the main process parameters is product yield ($Y_{X/S}$); it is yeast biomass. Fig. 7 shows that the yield of biomass for a rotary stirrer decreases twice and then remains approximately at the same level (slightly increases only during the third hour). In the case of vibromixing, the yield of biomass increases slowly; in the second hour it reaches the turbine process level, and then the curves of both of the processes have an approximately common tendency.⁴

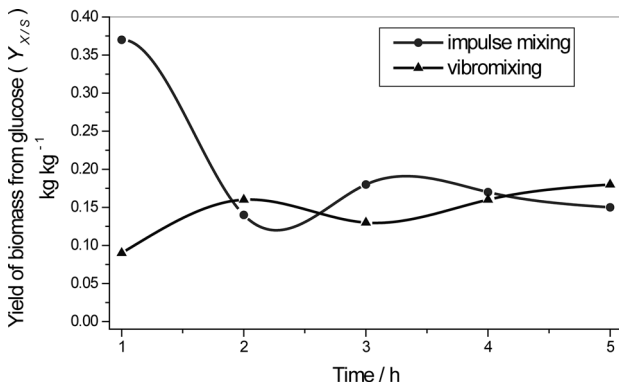


Fig. 7 – Yield of biomass from glucose ($Y_{X/S}$) growing the *Saccharomyces cerevisiae* in different mixing conditions

The results of this experiment show that in regard to the real fermentation processes, the process optimisation is even more important than the design of the mixing system.

Kinetic models

The mathematical model of the process for the impulse and vibromixing is based on the mass balance equations through perfect mixing in a bioreactor:

$$\begin{aligned} \frac{d\gamma_X}{dt} &= r_X \\ \frac{d\gamma_S}{dt} &= r_S \end{aligned} \quad (1)$$

The reaction rates for the cell and glucose are expressed as follows:

$$r_X = \mu \gamma_X, \text{ kg m}^{-3} \text{ h}^{-1}$$

and

$$r_S = -\frac{1}{Y_{X/S}} \mu \gamma_X, \text{ kg m}^{-3} \text{ h}^{-1}.$$

The initial conditions of the *impulse mixing* and *vibromixing* are:

impulse mixing:

$$\gamma_{X(0)} = 0.89 \text{ kg m}^{-3}, \quad \gamma_{S(0)} = 13.89 \text{ kg m}^{-3};$$

vibromixing:

$$\gamma_{X(0)} = 1.20 \text{ kg m}^{-3}, \quad \gamma_{S(0)} = 15.75 \text{ kg m}^{-3},$$

and

$$V_0 = 3 \cdot 10^{-3} \text{ m}^3.$$

The substrate inhibition occurs generally at high substrate concentrations. Different substrate inhibition models (*Monod, Aiba, Andrews, Haldane, Luong, Edward, and Han-Levenspiel*) are considered to explain the cell growth kinetics.^{15–17}

Evaluation of the model parameters

The mathematical estimation of the model parameters is based on the minimization of some quantities which can be calculated and which represent a function of the parameters to be estimated. If the model under consideration is linear, the estimation is generally an easy task. However, there is no general theory for nonlinear parameter estimation. The least-squares error is commonly used as a criterion for inspecting how close the computed profiles of the state variables are to the experimental observations.

We have used time as a weight factor for each experiment in the method of the smallest squares shown in this study. The criterion (Q_k) is expressed in the form below¹⁸:

$$\begin{aligned} Q_k = \frac{1}{N_S} \sum_{j=1}^{N_S} t_j \left(\frac{(\gamma_{X_e(t_j)} - \gamma_{X_m(t_j)})^2}{\gamma_{X_{e\max}}^2} + \right. \\ \left. + \frac{(\gamma_{S_e(t_j)} - \gamma_{S_m(t_j)})^2}{\gamma_{S_{e\max}}^2} \right) \end{aligned} \quad (2)$$

The least-squares regression sums up every observed error in (2) to yield an objective function. For parameter identification, we take the worst observed error of all experiments for an objective function. This approach is a special case of multiple objective parameter estimation of problems. The parameter estimation problem becomes a min–max problem¹⁸

$$\min_{\mathbf{x}} Q = \min_{\mathbf{x}} \max_k \{ Q_k, k = 1, \dots, N_{\text{exp}} \} \quad (3)$$

Models validation

The best dependences are defined by the statistical criteria: experimental correlation coefficient (R_E^2), experimental Fisher coefficient (F_E), relative error (S_L), and statistic 1 for different mixing systems of growth rate models. The statistic 1 has $F(M, N_{\text{exp}} - M)$ distribution. Statistic 1 is defined by¹⁹

$$\lambda = \frac{(N_{\text{exp}} - m) N_{\text{exp}}}{(N_{\text{exp}} - 1) M} \sum_{j=1}^M \frac{\Delta_j^2}{S_j} \quad (4)$$

where:

$$\Delta_{i,j}^2 = (\gamma_{X_e(i,j)} - \gamma_{X_m(i,j)})^2 + (\gamma_{S_e(i,j)} - \gamma_{S_m(i,j)})^2 ;$$

$$S_j = \frac{1}{N_{\text{exp}} - 1} \sum_{i=1}^{N_{\text{exp}}} (-\Delta_{i,j})^2 \Delta_j ;$$

$$\Delta_j = \frac{1}{N_{\text{exp}}} \sum_{i=1}^{N_{\text{exp}}} \sqrt{\Delta_{i,j}} , \text{ for } i = 1, N_{\text{exp}} \text{ and } j = 1, M.$$

The relative error (S_L) is determined by the following equation:

$$S_L = \sqrt{\frac{1}{(N_{\text{exp}} - M)}} \cdot \sqrt{\sum_{j=1}^{N_{\text{exp}}} \frac{(\gamma_{X_e(t_j)} - \gamma_{X_m(t_j)})^2}{\gamma_{X_e^2(t_j)}} + \frac{(\gamma_{S_e(t_j)} - \gamma_{S_m(t_j)})^2}{\gamma_{S_e^2(t_j)}}} \quad (5)$$

After identification of the parameters for growth rate models, the models (1) are compared to given statistical criteria. The model that has the best criteria values is used to the MOOP of the processes for the different mixing systems.

Multiple objective decision-making problems

The objective of the problem is to find optimal initial conditions of biomass ($\gamma_{X(0)}$), glucose concentration ($\gamma_{S(0)}$), maximal rotation speed (n_m) for *impulse mixing*, and maximal amplitude (A_m) for *vibromixing* where h? the following objective functions have maximum and minimum values

$$\begin{aligned} \max_{\mathbf{u}} J_1 &= V_0 (\gamma_{X(t_f)} - \gamma_{X(0)}) \\ \min_{\mathbf{u}} J_2 &= V_0 \gamma_{S(t_f)} \end{aligned} \quad (6)$$

The first objective function corresponds to biomass production. The second objective function corresponds to the residual of the glucose.

In order to define concisely the Pareto optimal solution, we have introduced the following definition^{8,10}

Definition 1. The feasible region in input space, W , is the set of all admissible control variables and the system parameters that satisfy the system constraints

$$\Omega = \{ \mathbf{u} \mid \dot{\mathbf{z}} = \mathbf{f}(\mathbf{z}, \mathbf{u}), \mathbf{z}(0) = \mathbf{z}_0 \text{ and } \mathbf{u}_{\min} \leq \mathbf{u} \leq \mathbf{u}_{\max} \}$$

where \mathbf{u}_{\min} and \mathbf{u}_{\max} are lower and upper bounded vectors of the control variables ($\mathbf{u}_1 \equiv \gamma_{X(0)}$, $\mathbf{u}_2 \equiv \gamma_{S(0)}$, $u_3 \equiv n_{\max}$ or A_{\max}). Here, the state equation $\dot{\mathbf{z}} = \mathbf{f}(\mathbf{z}, \mathbf{u})$ consists of batch model (1) for *impulse* or *vibromixing*.

We are now in a position to define Pareto optimal solutions in respect of the combined optimal control and optimal parameter selection problem.

Definition 2. The control action \mathbf{u}^* is a Pareto optimal policy, if and only if, $\mathbf{u} \in \Omega$ does not exist there:

$$\begin{aligned} J_i(\mathbf{u}) &\leq J_i(\mathbf{u}^*), \quad i = 1, 2 \\ J_k(\mathbf{u}) &< J_k(\mathbf{u}^*) \quad \text{for some } k \end{aligned}$$

In general, there are an infinite number of Pareto policies for a given MOOP. The collection of Pareto policies is the Pareto set. The image of this set is called the trade-off surface.

After the optimal solution is obtained through a multiple objective optimization technique, the second requirement in this decision-making problem is then performed to check whether the optimal solution satisfies the threshold values assigned. If the optimal solution does not satisfy the threshold values, the DM has to assign another threshold requirement. The problem should then be repeated to find another optimal solution. Interactive programming can be used to solve the decision-making problem. In this study, the interactive fuzzy optimisation is elaborated to solve the multiple objective optimal control and optimal parameter selection problem.

Fuzzy-decision-making problems

The optimal solution has to satisfy completely the assigned threshold values. It is assumed that the DM has fuzzy goals for each of the objective func-

tions (6). As a result, the DM considers that the fuzzy objective function J_1 should be substantially greater than or equal to the threshold interval $[J_1^L, J_1^U]$. The second goals should be substantially less than or equal to the assigned threshold interval $[J_2^L, J_2^U]$.

The multiple objective optimization problem (6) is now extended to the GMOOP given as

$$\text{fuzzy max}_{\mathbf{u}} J_1 = V_0 (\gamma_{\mathbf{x}(t_f)} - \gamma_{\mathbf{x}(0)}) \quad (7)$$

$$\text{fuzzy min}_{\mathbf{u}} J_2 = V_0 \gamma_{\mathbf{s}(t_f)} \quad (8)$$

The fuzzy requirement for each of the objective functions can be quantified by eliciting membership functions from the DM. Maximizing the fuzzy goal stated by the DM may achieve “*substantially greater than or equal to some intervals*”, and the DM is asked to determine the subjective membership function which is a strictly monotonically decreasing function compared to J_k . The linear membership functions are used in this study. The membership function for fuzzy maximizing goal (7) has the following type²⁰:

$$\nu_1(J_1) = \begin{cases} 0; & J_1(\mathbf{u}) \leq J_1^L \\ \frac{J_1(\mathbf{u}) - J_1^L}{J_1^U - J_1^L}; & J_1^L \leq J_1(\mathbf{u}) \leq J_1^U \\ 1; & J_1(\mathbf{u}) \geq J_1^U \end{cases} \quad (9)$$

The membership function for fuzzy minimizing goal (8) has the following type:

$$\nu_2(J_2) = \begin{cases} 1; & J_2(\mathbf{u}) \leq J_2^L \\ \frac{J_2(\mathbf{u}) - J_2^L}{J_2^U - J_2^L}; & J_2^L \leq J_2(\mathbf{u}) \leq J_2^U \\ 0; & J_2(\mathbf{u}) \geq J_2^U \end{cases} \quad (10)$$

The membership function for each of the objective functions is described in Fig. 7.

Having elicited the membership functions from the DM for each of the objective functions, the GMOOP (7)-(8) can be converted into the fuzzy multiple objective optimization problem (FMOOP) by aggregation of the criteria^{10,20}

$$\min_{\mathbf{u} \in \Omega} [\nu_1(J_1) \nu_2(J_2)]^T$$

By introducing a general aggregation operator $n_D(J_k)$, the fuzzy multiple objective decision-making problem (FMODMP) or maximizing decision problem can be defined by^{10,20}

$$\max_{\mathbf{u} \in \Omega} \nu_D \quad (11)$$

In this study, the fuzzy decision or minimum operator of Bellman and Zadeh¹⁹ is selected as aggregation operator:

$$\nu_D = \min_k \{ \nu_1(J_1), \nu_2(J_2) \}$$

Observe that the value of the aggregation operator can be interpreted as representing an overall degree of compliance with the DM’s multiple fuzzy goals. Let us consider the fuzzy maximizing problem. On the one hand, while the objective function value is greater than the assigned upper bound, such a solution absolutely satisfies the DM. On the other hand, the objective function value is smaller than the lower bound. It has to be rejected. As far as the objective function value is located in the threshold interval, the DM has satisfied the solution to some degree.

Fundamental to the MOOP (6) is the Pareto optimal concept. Therefore, the DM must select a compromise solution among the many Pareto optimal solutions. The relationships between the optimal solutions of (11) and the Pareto optimal concept of the MOOP can be characterized by the following theorem:^{10, 21}

Theorem 1. If \mathbf{u}^* is a unique optimal solution to the FMOOP (11), then \mathbf{u}^* is a Pareto optimal solution to the MOOP (6).

This theorem is used to guarantee that the unique optimal solution of (11) is a Pareto solution to the multiple objective optimal control problems (7)-(8). The statement of this theorem does not guarantee a unique optimal solution to (11).

Sakawa²¹ introduced the concept of fuzzy Pareto or M-Pareto optimal solutions for the general multiple objective nonlinear programming problems. Such a definition can be developed in regard to the combined optimal control and optimal parameter selection problem. This is defined by using membership functions objective functions.

Definition 3. If $\mathbf{u}^* \in \Omega$ is said to be an M-Pareto optimal solution to GMOOP and only if another $\mathbf{u}^* \in \Omega$ does not exist there, such that $\nu_k[J_k(\mathbf{u})] \geq \nu_k[J_k(\mathbf{u}^*)]$ will exist for all k and $\nu_j[J_j(\mathbf{u})] \neq \nu_j[J_j(\mathbf{u}^*)]$ – for at least one j .

Note that the set of Pareto optimal solutions is a subset of the set of M-Pareto optimal solutions as observed from Definitions 1, 2, and (9). Here, M refers to membership. Using the concept of M-Pareto optimality, the fuzzy version of Theorem 1 can be under slightly different conditions¹⁰.

Theorem 2. If \mathbf{u}^* is a unique optimal solution to the FMOOP (11), then \mathbf{u}^* is a Pareto optimal solution to the GMOOP (7)-(8).

Theorem 2 is used to guarantee that the unique optimal solution to the maximizing decision problem (11) is an M-Pareto optimal solution of fuzzy problems (7)-(8). The key point for using this theorem is to find a unique optimal solution to problem (11). A global optimization method has to be used to determine such a unique solution.

The proof of these theorems can be found in the publications of Wang¹⁰ and Sakawa.²¹

An algorithm and a program have been developed to find a satisfactory solution to the GMOOP. The algorithm is explained below:

1. Assigning the threshold intervals $[J_k^L, J_k^U]^r$.
2. Eliciting a membership function $v_k(J_k)$ from the DM for each of the objective functions.
3. Solving the maximizing decision problem (11). Let $[\mathbf{u}^r, \mathbf{v}_k^r(J_k)]$ be the M-Pareto optimal solution to the GMOOP (7)-(8).
4. If the DM is satisfied with the current levels of $\mathbf{v}_k^r(J_k)_{(k=1,2)}$, the current M-Pareto optimal solution $[\mathbf{u}^r, \mathbf{v}_k^r(J_k)]$ will be the satisfactory solution for the DM. Otherwise, the objectives are classified into three groups based on the DM's preference:

(a) a class of the objectives that the DM wants to improve,

(b) a class of the objectives that the DM may possibly agree to relax, and

(c) a class of the objectives that the DM accepts.

The index set of each class is represented by \mathbf{I}^r , \mathbf{R}^r , and \mathbf{A}^r , respectively. The new threshold intervals $[J_k^L, J_k^U]^{r+1}$ are reassigned in such a way that $[J_k^L, J_k^U]^r \subset [J_k^L, J_k^U]^{r+1}$ is for any $k \in \mathbf{I}^r$, $[J_k^L, J_k^U]^{r+1} \subset [J_k^L, J_k^U]^r$ for any $k \in \mathbf{R}^r$, and $[J_k^L, J_k^U]^{r+1} = [J_k^L, J_k^U]^r$ is for any $k \in \mathbf{A}^r$. Then Step 2 is repeated.

Here, it should be noted that any improvement for one of the objective functions could be achieved only at the expense of at least one of the other objective functions.

The programs developed were written using a COMPAQ Visual FORTRAN 90 Pro language. All computations were performed on AMD Athlon II X2 245, 2.9 GHz computer using Windows XP operating system.

Results and discussion

The reasoning mentioned above in regard to the two mixing systems suggests that, instead of seeking a mathematical description of the specific rates of the process using global models (models of specific rates in the entire time of cultivation), it is

more appropriate to seek different dependence relationships of the glucose. This is confirmed also by the initial structural identification of the specific growth rates. The identification of the growth rate models is not made separately from the decision of the model (1). It is done simultaneously by testing different dependencies. The parameters considered for the different growth rate models are given in Table 1. They are estimated using a developed algorithm and program.

The computing values of the statistical index are shown in Table 2.

Theoretical Fisher coefficient is $F_T(2, 4) = 6.256$, theoretical Fisher coefficient for statistic 1 is $F'_T(4, 2) = 6.944$, and theoretical correlation coefficient is $R^2_T(4) = 0.811$.²¹

The results obtained for correlation coefficient, Fisher coefficient, relative error and statistics 1 (Table 2), show that all growth rate models are adequate ($R^2_E > R^2_T$, $F_E < F'_T$, and Statistics $> F'_T$) and can be used for modelling processes for different mixing systems. The best statistical indexes for *impulse mixing* are shown by the *Luong* model (Table 1, Table 2). The results after simulations using the *Luong* model for biomass (g_x) and glucose concentrations (g_s) are presented in curves for *Saccharomyces cerevisiae* cultivation using *impulse mixing* (Fig. 8).

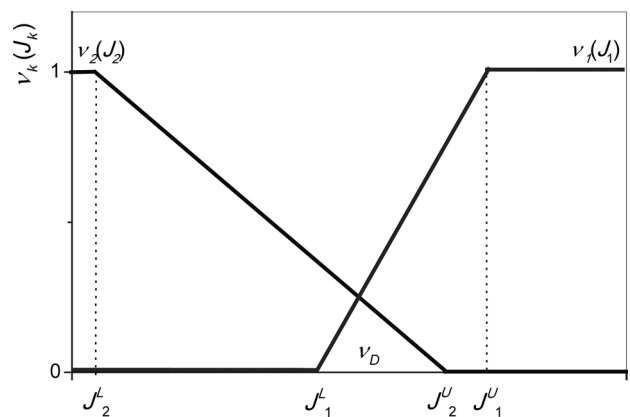


Fig. 8 – Membership function for each of the objective functions

For *vibromixing*, the criterion for minimization $\min Q$ (Table 1) has the lowest value for the *Haldane* model ($\min Q = 48.674 \cdot 10^{-5}$). Statistics 1 (Table 2) has the maximal value for the *Haldane* model. The correlation (R^2) and Fisher coefficients (F_E) have minimal differences for *Haldane* and *Luong* model (Table 2). The relative error (S_r) for *Luong* model is lower than *Haldane* model (Table 2). Therefore, we chose the *Luong* model for *vibromix-*

Table 1 – Estimated parameters of various growth rate models

Model	Equation	Parameters		$\min Q \cdot 10^{-5}$	
		impulse mixing	vibromixing	impulse mixing	vibromixing
Monod	$\mu = \frac{\mu_{\max} \gamma_S}{K_S + \gamma_S}$	$m_{\max} = 0.3305$ $K_S = 0.1736$ $Y_{X/S} = 0.1678$	$m_{\max} = 0.2389$ $K_S = 0.1000$ $Y_{X/S} = 0.1777$	73.199	67.288
Aiba	$\mu = \frac{\mu_{\max} \gamma_S}{K_S + \gamma_S} \exp\left(-\frac{\gamma_S}{K_I}\right)$	$m_{\max} = 0.4648$ $K_S = 0.8963$ $K_I = 39.2377$ $Y_{X/S} = 0.1691$	$m_{\max} = 0.3066$ $K_S = 0.4997$ $K_I = 54.2976$ $Y_{X/S} = 0.1771$	42.827	52.674
Andrews	$\mu = \frac{\mu_{\max} \gamma_S}{(K_S + \gamma_S) \left(1 + \frac{\gamma_S}{K_I}\right)}$	$m_{\max} = 0.4139$ $K_S = 0.6106$ $K_I = 52.7565$ $Y_{X/S} = 0.1683$	$m_{\max} = 0.3651$ $K_S = 0.8431$ $K_I = 26.5504$ $Y_{X/S} = 0.1771$	52.557	52.674
Haldane	$\mu = \frac{\mu_{\max} \gamma_S}{K_S + \gamma_S + \frac{\gamma_S^2}{K_I}}$	$m_{\max} = 0.4673$ $K_S = 0.9693$ $K_I = 31.0819$ $Y_{X/S} = 0.1685$	$m_{\max} = 0.4443$ $K_S = 1.4153$ $K_I = 15.3327$ $Y_{X/S} = 0.1771$	44.172	48.674
Luong	$\mu = \frac{\mu_{\max} \gamma_S}{K_S + \gamma_S} \left(1 - \frac{\gamma_S}{\gamma_S^*}\right)^n$	$m_{\max} = 0.7916$ $K_S = 3.2294$ $\gamma_S^* = 22.2013$ $n = 0.9092$ $Y_{X/S} = 0.1700$	$m_{\max} = 0.7323$ $K_S = 4.8893$ $\gamma_S^* = 21.8363$ $n = 0.9287$ $Y_{X/S} = 0.1781$	16.314	91.150
Edward	$\mu = \frac{\mu_{\max} \gamma_S}{K_S + \gamma_S + \left(\frac{\gamma_S^2}{K_{SI}}\right) \left(1 + \frac{\gamma_S}{K}\right)}$	$m_{\max} = 0.4798$ $K_S = 1.0685$ $K_{SI} = 38.0981$ $K = 34.3451$ $Y_{X/S} = 0.1691$	$m_{\max} = 0.3843$ $K_S = 1.0673$ $K_{SI} = 29.6737$ $K = 33.7743$ $Y_{X/S} = 0.1771$	37.596	52.674
Han-Levenspiel	$\mu = \mu_{\max} \left(1 - \frac{\gamma_S}{\gamma_S^*}\right)^n \frac{\gamma_S}{\gamma_S + C_M \left(1 - \frac{\gamma_S}{\gamma_S^*}\right)^m}$	$m_{\max} = 0.5839$ $\gamma_S^* = 27.7536$ $C_M = 1.7444$ $n = 0.8822$ $m = 0.1597$ $Y_{X/S} = 0.1698$	$m_{\max} = 0.3453$ $\gamma_S^* = 19.0112$ $C_M = 0.8449$ $n = 0.2980$ $m = 0.0305$ $Y_{X/S} = 0.1771$	24.535	52.858

ing. Thus, both mixing systems have the same growth rate models. The difference between *Haldane* and *Luong* models is insignificant and clearly seen in Fig. 9, which shows the results after simulations of biomass (g_X) and glucose concentrations (g_S) for *Saccharomyces cerevisiae* cultivation using *vibromixing* conditions for *Haldane* and *Luong* models.

The model of the processes (1) for both mixing systems has the following form:

$$\begin{aligned} \frac{d\gamma_X}{dt} &= \frac{\mu_{\max} \gamma_S}{K_S + \gamma_S} \left(1 - \frac{\gamma_S}{\gamma_S^*}\right)^n \gamma_X \\ \frac{d\gamma_S}{dt} &= -\frac{1}{Y_{X/S}} \frac{\mu_m \gamma_S}{K_S + \gamma_S} \left(1 - \frac{\gamma_S}{\gamma_S^*}\right)^n \gamma_X \end{aligned} \quad (12)$$

Table 2 – Statistical index values

Statistical index		R_E^2				F_E			
systems		impulse mixing		vibromixing		impulse mixing		vibromixing	
No	Models	X	S	X	S	X	S	X	S
1	<i>Monod</i>	0.9982	0.9985	0.9971	0.9994	1.0290	1.0060	1.0473	1.0145
2	<i>Aiba</i>	0.9988	0.9991	0.9981	0.9985	1.0182	1.0036	1.0313	0.9957
3	<i>Andrews</i>	0.9986	0.9989	0.9983	0.9983	1.0245	1.0049	1.0294	0.9938
4	<i>Haldane</i>	0.9988	0.9991	0.9986	0.9994	1.0237	1.0052	1.0187	0.9875
5	<i>Luong</i>	0.9994	0.9997	0.9972	0.9991	1.0093	0.9965	1.0264	0.9889
6	<i>Edward</i>	0.9989	0.9992	0.9982	0.9993	1.0183	1.0034	1.0260	0.9906
7	<i>Han-Levenspiel</i>	0.9992	0.9994	0.9981	0.9992	1.0117	1.0012	1.0229	0.9903

Statistical index		S_L				Statistic λ	
systems		impulse mixing		vibromixing		impulse mixing	vibromixing
No	models	X	S	X	S		
1	<i>Monod</i>	0.0481	0.6081	0.0605	0.0378	109956	17302
2	<i>Aiba</i>	0.0385	0.5652	0.0484	0.1667	259986	39092
3	<i>Andrews</i>	0.0364	0.5983	0.0437	0.1666	186131	53005
4	<i>Haldane</i>	0.0297	0.5617	0.0366	0.1675	235709	87643
5	<i>Luong</i>	0.0211	0.4849	0.0284	0.0983	1373534	53775
6	<i>Edward</i>	0.0363	0.5550	0.0362	0.1673	343001	83206
7	<i>Han-Levenspiel</i>	0.0295	0.5311	0.0325	0.1610	618070	84510

The parameters in model (12) are:

Mixing systems	μ_m	K_S	$Y_{X/S}$	n	γ_S^*
Impulse mixing	0.79 h ⁻¹	3.23 kg m ⁻³	0.17 kg kg ⁻¹	0.91	22.20 kg m ⁻³
Vibro-mixing	0.73 h ⁻¹	4.89 kg m ⁻³	0.18 kg kg ⁻¹	0.93	21.84 kg m ⁻³

Further herein, we will determine the global optimal solutions.

Determining of the global optimal solution

In order to obtain a global optimal solution, an FST method^{20,23,24} was introduced to solve the maximizing decision problem (11). A simple guideline is presented in the interactive programming procedures in order to find a satisfactory solution to the FMODMP. The function used to determine a global solution is defined as

$$\beta_0 \cong \underset{u}{\text{m}\ddot{\text{a}}\text{x}} v_D \quad (13)$$

where: „m $\ddot{\text{a}}$ x” means „in possibility maximum”, „ \cong ” means „has come into view approximately in following relation”.

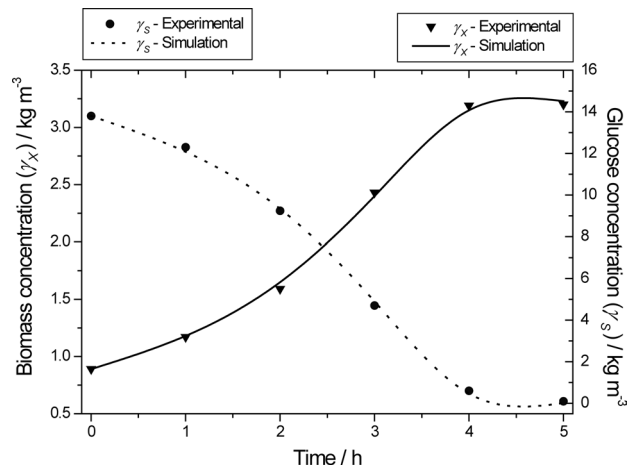


Fig. 9 – Experimental and simulation results using the impulse mixing system

Fuzzy sets theory²⁰ allows development of a “flexible” model that reflects in more detail all possible values of the criterion and control variables under the model developed. The model of the processes (12) for *impulse mixing* and *vibromixing* is considered the most appropriate, but deviations are admissible with a small degree of acceptance. It is represented by a fuzzy set of the following type γ_X

and γ_S for different mixing systems and has come into view approximately by the following relations

$$\beta_i(\mathbf{u}) = \frac{1}{1 + \varepsilon_i^2}, \quad i = 1, 2 \quad (14)$$

where:

$$\varepsilon_1 = \frac{d\gamma_X}{dt} - \mu\gamma_X, \quad \varepsilon_2 = \frac{d\gamma_S}{dt} + \mu\gamma_X / Y_{X/S}.$$

The propositional “flexible” model of the process reflects better influence of all good values of the kinetics variables. The “flexible” model reflects in more detail all possible values of the criterion and control variables under the model developed. After examination, the model is considered the most acceptable.

The fuzzy set of the solution is presented with a membership function of the criteria β_0 and model b_1 and b_2 for different mixing systems^{23,24}

$$\beta_D(\mathbf{u}) = (1 - \xi) \prod_{i=0}^2 \beta_i^{\theta_i}(\mathbf{u}) + \xi \left\{ 1 - \prod_{i=0}^2 [1 - \beta_i(\mathbf{u})]^{\theta_i} \right\} \quad (15)$$

This was obtained by using the common defuzzification method BADD²⁵

$$\mathbf{u}^0 = \sum_{i=1}^q \frac{\beta_{D_i}^{\theta_i}(\mathbf{u}) \mathbf{u}_i}{\sum_{j=1}^p \beta_{D_j}^{\theta_j}(\mathbf{u})}, \quad i = 1, \dots, q; \quad j = 1, \dots, p; \quad p = q^m \quad (16)$$

This method allows direct (non-iterative) determination of the optimization problem.

The control variables are satisfied in the following intervals:
initial condition

$$[0.80 = u_{\min_1} \leq u_1 \leq u_{\max_1} = 1.5] \text{ kg m}^{-3},$$

and

$$[13.0 = u_{\min_2} \leq u_2 \leq u_{\max_2} = 17.0] \text{ kg m}^{-3};$$

rotation speed for *impulse mixing*

$$[240 = u_{\min_3} \leq u_3 \leq u_{\max_3} = 280] \text{ rpm},$$

or amplitude for *vibromixing*

$$[8.0 = u_{\min_3} \leq u_3 \leq u_{\max_3} = 12.0] \cdot 10^{-3} \text{ m}.$$

The assigned threshold interval and the optimal membership function value for each objective function are

Objective	1 st	2 nd
$[J_k^L \quad J_k^U]$	$[8 \cdot 10^{-3} \text{ kg}$ $12 \cdot 10^{-3} \text{ kg}]$	$[0.01 \cdot 10^{-3} \text{ kg}$ $0.50 \cdot 10^{-3} \text{ kg}]$
Impulse mixing, $v_k^*(J_k)$	0.268	0.752
Vibromixing, $v_k^*(J_k)$	0.155	0.879

Now, the global solution (13) can be obtained by (14)-(16). By choosing 15 time partition for all the control variables $\gamma_{X(0)}$, $\gamma_{S(0)}$, n_m or A_m , have to be determined in the finite-dimensional optimization problem.¹⁰ The values elected for the parameters that characterize the compensation degree (ξ), and weights of $\beta(\mathbf{u})$ are $\xi = 0.95$, $\theta_0 = 1$, and $\theta_{i(i=1,2)} = 0.9$, respectively.

Table 3 shows the optimal membership function value for each of the objective functions as well as the optimal values of the control variable of the batch cultivation of *Saccharomyces cerevisiae*. Stage 0 shows the process before optimisation, Stage 1 – after optimisation with different initial conditions, Stage 2 – after optimisation with different optimal initial conditions (after Stage 1), and Stage 3 shows the membership function value for

Table 3 – Results after multiple optimisation of *Saccharomyces cerevisiae* batch cultivation

Impulse mixing								
Stage	u_1^0 kg m ⁻³	u_2^0 kg m ⁻³	u_3^0 rpm	β_0 –	J_1 kg	$v_1^*(J_1)$ –	J_2 kg	$v_2^*(J_2)$ –
0	0.89	13.80	260	0.000	$7.04 \cdot 10^{-3}$	0.000	$16.00 \cdot 10^{-6}$	0.013
1	1.45	15.69	211	0.997	$9.87 \cdot 10^{-3}$	0.290	$4.00 \cdot 10^{-6}$	0.882
2	1.43	14.00	177	0.973	$8.80 \cdot 10^{-3}$	0.199	$1.00 \cdot 10^{-6}$	0.714
3	1.42	13.75	177	0.573	$10.29 \cdot 10^{-3}$	0.573	$5.60 \cdot 10^{-6}$	0.706
Vibromixing								
0	1.20	15.75	10.0	0.000	$8.02 \cdot 10^{-3}$	0.005	$2.23 \cdot 10^{-3}$	0.000
1	1.35	13.33	8.3	0.954	$8.63 \cdot 10^{-3}$	0.156	$0.47 \cdot 10^{-3}$	0.890
2	1.41	13.50	8.0	0.783	$8.75 \cdot 10^{-3}$	0.188	$0.35 \cdot 10^{-3}$	0.827
3	1.42	13.75	8.0	0.268	$9.08 \cdot 10^{-3}$	0.269	$0.49 \cdot 10^{-3}$	0.971

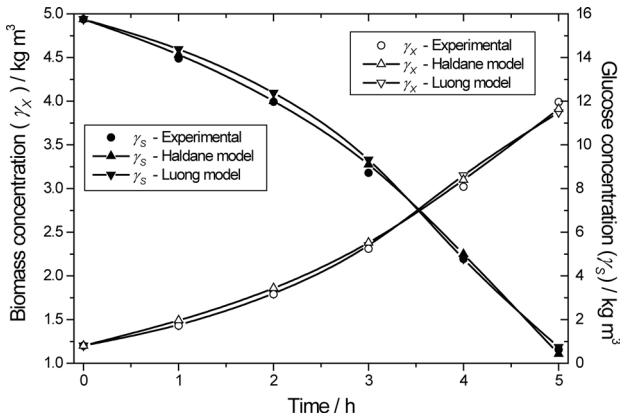


Fig. 10 – Experimental and simulation results using the vibromixing system

each of the objective functions with identical initial conditions for both systems.

The optimisation results (Table 3 – Stage 1) have shown that the biomass concentration increases by more than 45 % for *impulse mixing* and only by 9 % for *vibromixing*. The glucose concentration decreases by more than 70 % in the *impulse mixing* and more than 80 % in the *vibromixing*. These results indicate that the biomass production ($J_1 = 9.87 \cdot 10^{-3}$ kg) in the *impulse mixing* process is better than that in the *vibromixing* ($J_1 = 8.63 \cdot 10^{-3}$ kg), and the residual glucose concentration is also much better (*impulse mixing* $J_2 = 4.00 \cdot 10^{-6}$ kg) than the one in the *vibromixing* ($J_2 = 0.47 \cdot 10^{-3}$ kg).

The results for the biomass and glucose concentrations for different mixing systems before and after optimisation are shown in Fig. 11 and Fig. 12.

The results shown in Fig. 11 and Fig. 12 are related to different initial optimal conditions.

It is interesting to determine what the optimal values of the objective functions for identical initial conditions will be.

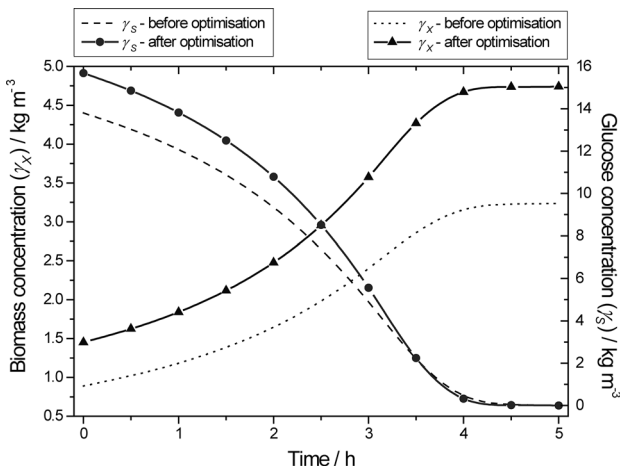


Fig. 11 – Results before and after optimisation for impulse mixing systems

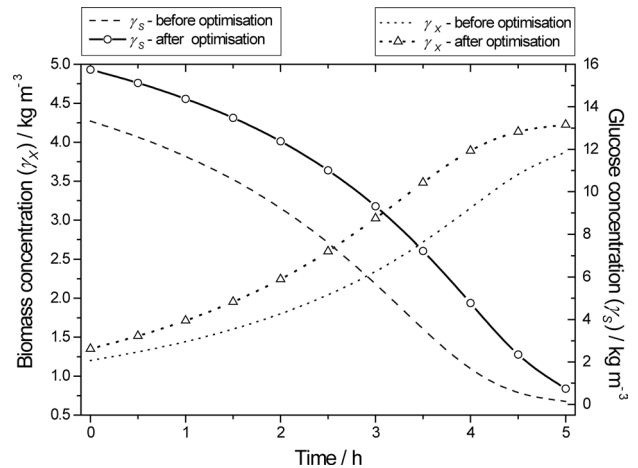


Fig. 12 – Results before and after optimisation for vibromixing systems

The initial conditions are examined within the optimum values [$1.35 \text{ kg m}^{-3} \leq u_1 \leq 1.45 \text{ kg m}^{-3}$] and [$13.33 \text{ kg m}^{-3} \leq u_2 \leq 15.69 \text{ kg m}^{-3}$]. The maximal rotation speed ($n_m = 210.72 \text{ rpm}$) for *impulse mixing*, the amplitude ($A_m = 8.17 \cdot 10^{-3} \text{ m}$) for *vibromixing*, and the threshold interval are not changed.

FDMOOP (11) and the maximizing decision problem (13)-(16) are solved again for these intervals of the control variables.

The results show (Table 3 – Stage 2) that the biomass concentration decreases by more than 8 % for *impulse mixing* and increases by 2.5 % for *vibromixing*. The glucose concentration decreases by more than 80 % in *impulse mixing* and by more than 20 % for *vibromixing*. These results show that, for *impulse mixing*, the biomass production decreases (around 0.02 %) and there is significant improvement of the residual of glucose (more 80 %). For *vibromixing*, we have improvement of both objective functions. The biomass production increases by 2.5 % and the residual glucose concentration decreases by more than 20 %. The difference in the biomass production of both systems does not differ significantly (around 0.5 %).

The results (Table 3 – Stages 1 and 2) show that both mixing systems can and must be with the same initial conditions (mean values between Stage 1 and Stage 2), i.e. $\gamma_{X(0)} = 1.42 \text{ kg m}^{-3}$ and $\gamma_{S(0)} = 13.75 \text{ kg m}^{-3}$. Under these conditions, the optimization problem was solved again. The maximal rotation speed (n_m) or amplitude (A_m) were changed in wider intervals $u_3 \in [100 \text{ rpm} \div 280 \text{ rpm}]$, or $u_3 \in [6 \cdot 10^{-3} \text{ m}, 12 \cdot 10^{-3} \text{ m}]$. The results are shown in Table 3 – Stage 3. These results show that the biomass concentration increases by more than 12 % for *impulse mixing* and increases only by 1.31 % for *vibromixing*. The glucose concentration increases more than 8-fold for *impulse mixing* and by more than 18 % in

vibromixing. The results also show that, in *impulse mixing*, the biomass production increases by more than 17 % and residual glucose increases 8-fold at the end of the process. The results for *vibromixing* are similar in biomass production (about 4 %) and the residual glucose concentration decreases by more than 37 %. The improvement of the objective function (J_1) leads to a change in another objective function (J_2).

The results for the biomass and glucose concentrations for different mixing systems after optimisation with identical initial conditions are shown in Fig. 13 and Fig. 14.

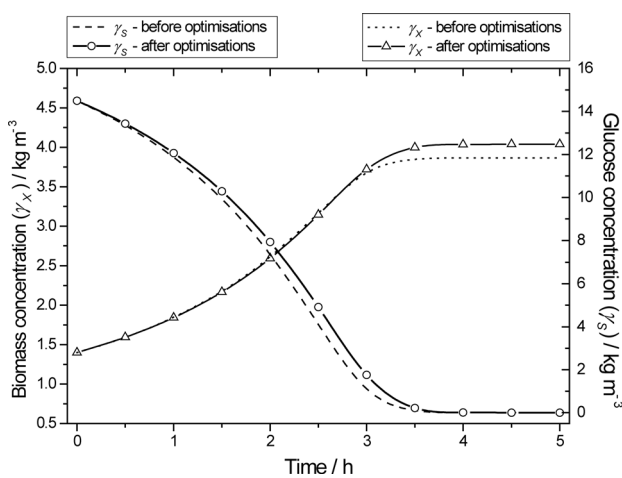


Fig. 13 – Results after optimisation with identical initial conditions for *impulse mixing* systems

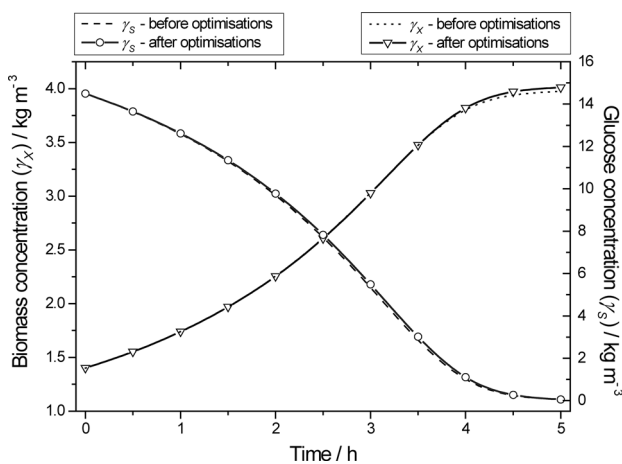


Fig. 14 – Results after optimisation with identical initial conditions for *vibromixing* systems

The obtained results show that *impulse mixing* is preferable to *vibromixing*. Another advantage is that expensive special equipment is not required. It can be realized easily in any bioreactor having control systems equipped with a generator for a saw impulse.

Conclusions

1. The present results show that the *Luong* growth rate model proposed seems to be useful for representing the kinetics of substrate inhibition in *impulse mixing* and *vibromixing*. This model is of a generalized Monod type, but it accounts for substrate stimulation at low and high concentrations. The model has the capability to predict the values of critical inhibitor concentration. When their maximum value is reached, the reactions stop.

2. In comparison to traditional continuous mixing, *impulse* and *vibromixing* decrease the ability of cells to present themselves in the local intensive zone in similar mixing conditions. In the *Saccharomyces cerevisiae* fermentation, a higher maximum growth rate is achieved by *impulse mixing* rather than with *vibromixing*. However, a similar process yield is reached in the case of *vibromixing*. Having reached a certain biomass density, *impulse mixing* starts to affect cell growth. This means that at a greater biomass density, sufficient prevention of the presence of cells in locally intensive zones is not possible.

3. The results achieved after the multiple optimisation of *Saccharomyces cerevisiae* batch cultivation for different mixing systems, show a significant increase in biomass concentration, and respectively an increase in biomass production. It also significantly reduces the residual glucose concentration. After solving again the fuzzy-decision-making problem and finding the global solution by the previously established values of optimal control variables, the results show that the biomass concentration decreases for *impulse mixing* and increase for *vibromixing*. The glucose concentration decreases for both mixing systems. Finally, in regard to the identical initial conditions, the results have shown that the biomass concentration increases for *impulse mixing* and *vibromixing* systems. The glucose concentration increases more than 8-fold for *impulse mixing* and by more than 18 % for *vibromixing*. Here, it should be noted that, any improvement for one of the objective functions, can be achieved only at the expense of at least one of the other objective functions. These results indicate that the biomass production in the process of *impulse mixing* is better than that in *vibromixing*. The residual glucose concentration is also much better. In addition, this system is easier to realize. Let us keep in mind that the results are theoretical and they have not been confirmed by experiments.

4. The applied multiple objective optimisation of the process has shown a vast increase in productivity, and respectively a decrease in the residual of the glucose concentration. This result leads to higher effectiveness for each of them. The results of this investigation show that the optimisation of the process is more important for real fermentation processes than for the design of mixing systems.

Nomenclature

A_m – maximal amplitude for *vibromixing*, m
 C_M – Monod's constant, kg m⁻³
 D – diameter of bioreactor, m
 f – frequency, s⁻¹
 J_k – objective functions, kg
 J_k^L, J_k^U – low and upper values of objective functions, kg
 K – constant in *Edward* model
 K_P, K_{SI} – inhibition constants, kg m⁻³
 K_S – saturation coefficient, kg m⁻³
 M – number of kinetics variables, $M = 2$
 m – constant which accounts the relationship between C_M and γ_S
 n – constant which accounts the relationship between μ and g_s
 N_{exp} – number of experiments
 n_m – maximal rotation speed, rpm
 N_S – number of sampling data
 \min_Q – criterion for parameters identification in the \mathbf{x} growth rate models, –
 q – number of discrete values of vector \mathbf{u}
 r – r – axis, m
 r_S – glucose consumption rate, kg m⁻³ h⁻¹
 R_S – specific glucose consumption rate, h⁻¹
 r_X – growth of biomass rate, kg m⁻³ h⁻¹
 T – period, s
 t_j – glucose at sampling time, h
 t_f – final process time, h
 \mathbf{u} – vector of control variables,
 $\mathbf{u} = \mathbf{u}[\gamma_{X(0)}, \gamma_{S(0)}, n_{max} \text{ or } A_{max}]^T$
 \mathbf{u}_{min} and \mathbf{u}_{max} – lower and upper bounded vectors of the control variables
 \mathbf{u}^* – optimal values of control variables, after M-Pareto optimal solutions
 \mathbf{u}^0 – global optimal values of control variables
 V_0 – initial liquid volume, m³
 \mathbf{x} – vector of estimated parameters in growth rate models,
 $\mathbf{x} = [m_{max}, K_S, K_{SI}, K_P, \dots]^T$
 $Y_{X/S}$ – yield coefficient, kg kg⁻¹
 z – z – axis, m

Greek letters

$\beta_0(\mathbf{u})$ – membership function for solution to the maximizing decision problem
 $\beta_i(\mathbf{u})$ – membership function for the model ($i = 1, 2$)
 γ – mass concentration, kg m⁻³
 γ_X – biomass mass concentration, kg m⁻³
 $\gamma_X(0)$ – biomass initial mass concentration, kg m⁻³
 γ_S – glucose mass concentration, kg m⁻³
 γ_S^* – critical inhibitor concentration, above which the reactions stop, kg m⁻³
 $\gamma_S(0) = \gamma_{S_0}$ – glucose initial mass concentration, kg m⁻³

$\gamma_{Xe(t_j)}, \gamma_{Se(t_j)}$ – the measured data at $t = t_j$
 $\gamma_{Xm(t_j)}, \gamma_{Sm(t_j)}$ – concentrations calculated using the model, kg m⁻³
 $\gamma_{Xe_{max}}, \gamma_{Se_{max}}$ – maximal measured concentrations, kg m⁻³
 ξ – parameter characterizing the compensation degree
 μ – specific growth rate of cell culture from glucose, h⁻¹
 μ_m – maximum specific growth rate of cell culture from glucose, h⁻¹
 ν_D – general aggregation operator
 ε_i – deviations of the basic model
 θ_i – parameters, those give weight of $b_i(\mathbf{u})$
 χ_i – weight coefficients
 $\nu_k(J_k)$ – membership function for each objective function
 Ω – feasible region in input space

Abbreviations

BADD – Basic Defuzzification Distributions
 DM – Decision Making
 FMODMP – Fuzzy Multiple Objective Decision-Making Problem
 FMOOP – Fuzzy Multiple Objective Optimization Problem
 FST – Fuzzy Sets Theory
 GMOOP – General Multiple Objective Optimization Problem
 MOOP – Multiple Objective Optimization Problem
 SCADA – Supervisory Control and Data Acquisition

References

1. Kafarov, V., Vinarov, A., Gordeev, L., Modelling Biochemical Reactors, Moscow, Lesnaya promishlenost, 1979, pp.179 – 296 (in Russian).
2. Vanags, J., Rikmanis, M., Ushkans, E., Viesturs, U., Stirring characteristics in bioreactors, *AIChE J.* **36** (1990) 1361. <http://dx.doi.org/10.1002/aic.690360909>
3. Viestur, U., Kuznetsov, A., Savenkov, V., Systems Fermentation, Riga, Zinatne, 1986, pp. 90 – 127 (In Russian).
4. Viesturs, U., Berzins, A., Vanags, J., Tzonkov, St., Ilkova, T., Petrov, M., Pencheva, T., Application of different mixing systems for the batch cultivation of the *Saccharomyces cerevisiae*. Part I: Experimental investigations and modelling, *Int. J. Bioautomation* **13**(2) (2009) 45.
5. Sendin, O., Vera, J., Nestor, T., Model based optimization of biochemical systems using multiple objectives: A comparison of several solution strategies, *Math. and Comp. Model. Dyn.* **12**(5) (2006) 469. <http://dx.doi.org/10.1080/13873950600723442>
6. Sergienko, I., Parasyuk, N., Kaspshitskaya, M., A fuzzy problem of multiparametric choice of optimal solutions, *Cybern. and Syst. Anal.* **39** (2003) 163. <http://dx.doi.org/10.1023/A:1024731004624>
7. Vera, J., de Atauri, P., Cascante, M., Torres, NV, Multicriteria optimization of biochemical systems by linear programming. Application to the ethanol production by *Saccharomyces cerevisiae*, *Biotechnol. and Bioeng.* **83**(3) (2003) 335. <http://dx.doi.org/10.1002/bit.10676>

8. Zhou, Y. H., Titchener-Hooper, N. J., The application of a Pareto optimisation method in the design of an integrated bioprocess, *Bioprocess and Biosyst. Eng.* **25** (2003) 349. <http://dx.doi.org/10.1007/s00449-003-0318-0>
9. Tonon, F., Bernardini, A., Multiobjective optimization of uncertain structures through fuzzy sets and random set theory, *Comput.-Aided Civ. Inf.* **14** (1999) 119. <http://dx.doi.org/10.1111/0885-9507.00135>
10. Wang, F.-S., Chang-Huei, J., Fuzzy-decision-making problems of fuel ethanol production using a genetically engineered yeast, *Ind. and Eng. Chem. Res.* **37** (1998) 3434. <http://dx.doi.org/10.1021/ie970736d>
11. Petrov, M., Ilkova, T., Fuzzy optimization of biosynthesis of *L-lysine*, *Chem. Biochem. Eng. Q.* **19**(3) (2005) 283.
12. Petrov, M., Multiple objective optimization and optimal control of fermentation processes, *Int. J. Bioautomation* **10** (2008) 21.
13. Vanags, J., Rychtera, M., Ferzik, S., Vishkins, M., Viesturs, U., oxygen and temperature control during the cultivation of microorganisms using substrate feeding, *Eng. in Life sci.* **7**(3) (2007) 247. <http://dx.doi.org/10.1002/elsc.200620184>
14. Vanags, J., Viesturs, U., Bērziņš, A., Performance of the cultivation of microorganisms using different mixing systems, 18th Int. Congress of Chem. and process Eng. – CHISA'08, Summaries 3. Systems and Technology, 24-28 august 2008, prague, Czech republic. p. 851, CDROM full text 1-8.
15. Gera, N., Uppaluri, R. V. S., Sen, S., Venkata Dasuc, V., Growth kinetics and production of glucose oxidase using *Aspergillusniger* NRRL326, *Chem. Biochem. Eng. Q.* **22**(3) (2008) 315.
16. Namjoshi, A., Ramkrishna, D., Multiplicity and stability of steady states in continuous bioreactors: Dissection of cybernetic models, *Chem. Eng. Sci.* **56**(19) (2001) 593. [http://dx.doi.org/10.1016/S0009-2509\(01\)00166-X](http://dx.doi.org/10.1016/S0009-2509(01)00166-X)
17. Chen, Y., Wang, F.-S., Crisp and fuzzy optimization of a fed-batch fermentation for ethanol production, *Ind. Eng. Chem. Res.* **42** (2003) 6843. <http://dx.doi.org/10.1021/ie0210107>
18. Wang, F.-S., Tzu-Liang, Su, Horng-Jhy, J., Hybrid differential evolution for problems of kinetic parameter estimation and dynamic optimization of an ethanol fermentation process, *Ind. Eng. Chem. Res.* **40** (2001) 2876. <http://dx.doi.org/10.1021/ie000544+>
19. Giridhar, R., Srivastava, A. K., Model based constant feed fed-batch *L-Sorbose* production process for improvement in *L-Sorbose* productivity, *Chem. Biochem. Eng. Q.* **14**(4) (2000) 133.
20. Bellman, R., Zadeh, L., Decision making in a fuzzy environment, *Manage. Sci.* **17**(4) (1970) B141. <http://dx.doi.org/10.1287/mnsc.17.4.B141>
21. Sakawa, M., Fuzzy Sets and Interactive Multiobjective Optimization, Plenum Press, New York, 1993. <http://dx.doi.org/10.1007/978-1-4899-1633-4>
22. Stoyanov, S., Optimization Methods and Algorithms, Technique, Sofia, 1990, pp.391 – 398 (in Bulgarian).
23. Angelov, P., An analytical method for solving a type of fuzzy optimization problems, *Control and Cybern.* **24**(3) (1995) 363.
24. Angelov, P., Generalized approach to fuzzy optimization, *Int. J. of Intell. Sys.* **9**(3) (1994) 261. <http://dx.doi.org/10.1002/int.4550090302>
25. Filev, D., Yager, R., A generalized defuzzification method via bad distribution, *Int. J. of Intell. Sys.* **6** (1991) 687. <http://dx.doi.org/10.1002/int.4550060702>